PROCEEDINGS OF SCIENCE

Development of a Pressurized Helium Scintillating Calorimeter for AntiMatter Identification

L.E. Ghezzer,[1,2] **G. Giovanazzi,**[1,2] **F. Nozzoli,**[2,1,*] **L. Ricci,**[1] **F. Rossi,**[1,2] **P. Spinnato,**[2] **E. Verroi,**[2] **P. Zuccon,**[1,2] **F. Bruni**[3,4] **and F. Meinardi**[3,4]

[1] *Dipartimento di Fisica, Università di Trento, Trento Italy*

[2] *INFN - Trento Institute for Fundamental Physics and Applications, Trento Italy*

[3] *Dipartimento Scienza dei Materiali, Università di Milano Bicocca, Milano Italy*

[4] *Glass to Power s.p.a., Via Fortunato Zeni 8, Rovereto, Italy*

E-mail: Francesco.Nozzoli@unitn.it

The detection of low-energy antideuterons in Cosmic Rays (CRs) addresses crucial questions regarding the antimatter asymmetry in the Universe and the potential identification of annihilating Dark Matter particles in the galactic halo. The Pressurized Helium Scintillating Calorimeter for AntiMatter Identification (PHeSCAMI) project aims to explore a novel signature for identifying antideuterons and antiprotons in CRs through delayed annihilations within a helium target. We present the performance evaluation of a large-acceptance detector design for PHeSCAMI, including the development of a possible trigger logic and the estimation of the expected background rate using Monte Carlo simulations based on the Geant4 toolkit. Additionally, we investigate the performance of the FB118 Wavelength Shifter (WLS), manufactured by "Glass to Power", in a two-stage system designed to convert VUV (80 nm) scintillation light from the helium into visible light.

International Conference on Exotic Atoms and Related Topics and Conference on Low Energy Antiprotons (EXA-LEAP2024)
26-30 August 2024
Austrian Academy of Sciences, Vienna.

*Speaker

 ISSN 1824-8039 . Published by SISSA Medialab.

PoS(EXA-LEAP2024)048

1. The PHeSCAMI detector

The study of low-energy antideuterons ($\bar{d}$) in cosmic rays (CRs) presents a valuable method for searching for dark matter (DM) annihilation and primordial antimatter in our galaxy. Research conducted by the PHENIX [1] and ALICE [2] collaborations indicate that the production of low-energy antideuterons as secondary particles during cosmic ray propagation is improbable. This indicates a minimal astrophysical background in the search for complex antinuclei within CRs. Consequently, detecting low-energy antideuterons serves as a prime channel for identifying DM annihilation or the presence of primordial antimatter. The Pressurized Helium Scintillating Calorimeter for AntiMatter

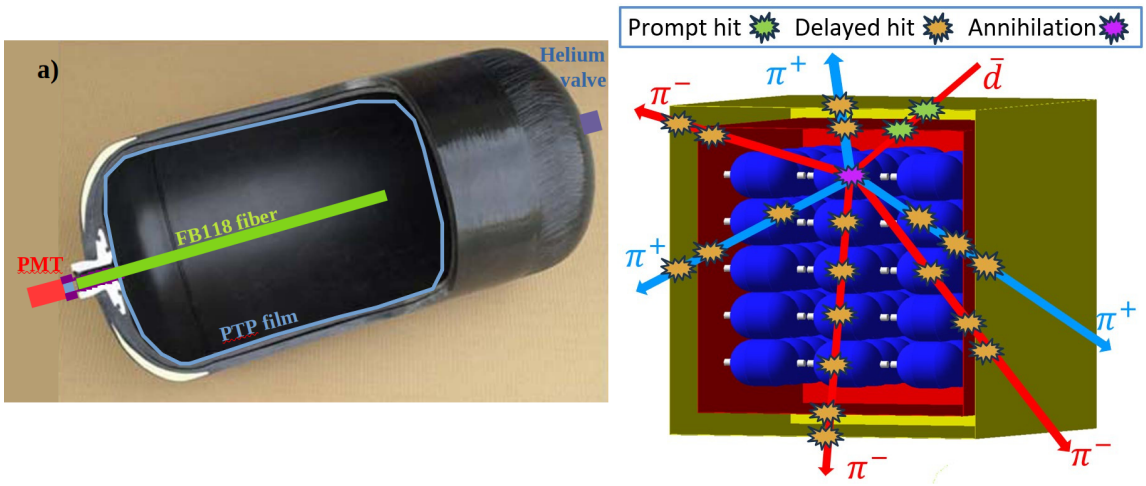

Figure 1: Left: proposed design of a single Helium Calorimeter (HeCal) tank with the two-stage WLS system that convert He scintillation light (80 nm) to visible light for PMT collection. Right: the simulated design of PHeSCAMI detector composed by a Time of Flight (TOF) system made by segmented plastic scintillators (red and yellow) and the HeCal composed of 75 space-qualified helium tanks (blue). The figure depicts an antideuteron ($\bar{d}$) annihilation, where the green markers denote prompt energy depositions occurring within a few nanoseconds, and the yellow markers indicate delayed depositions resulting from the annihilation.

Identification (PHeSCAMI) project aims to identify low-energy antideuterons by utilizing delayed annihilations within a helium target. When Z=-1 antinuclei stop in helium, they can form exotic atoms in a meta-stable state [3]. Approximately 3.3% of these meta-stable states have a long lifetime (μs) leading to a detectable delay of the annihilation. The PHeSCAMI detector is designed to identify such Z=-1 antinuclei in CRs through this signature. The proposed detector design consists of two main components: a Time of Flight system (TOF) and a segmented Helium Calorimeter (HeCal). The TOF system is constructed from two cubic layers of segmented plastic scintillators, with each face of the cube composed of 64 slabs, 0.4 cm thick, and the distance between the external and internal TOF layers being 20 cm. The HeCal comprises 75 carbon-fiber helium tanks, each filled with 50 liters of helium pressurized at 310 bar, which acts as a fast scintillator with a time resolution generally below 300 ps [3]. The helium tanks' mass and structural design are in line with state-of-the-art parameters for space-qualified pressurized helium tanks. [4]. Due the fact that Helium scintillator emits in the 80 nm range [5], scintillation photons needs to be downshifted before being collected by the PMT, in Fig.1 (left) the design of a single HeCal tank is showed, with a Wavelength Shifter (WLS) system inspired by the DUNE experiment [6]. Fig.1 (right)

illustrates a possible design of the PHeSCAMI detector, showing an example of an antideuteron undergoing delayed annihilation within the HeCal. The prompt hits, depicted in green, indicate energy depositions within a few nanoseconds produced by the antideuteron slowing down in the TOF and stopping in the helium. The delayed hits, depicted in yellow, show energy depositions from several $\pi^{\pm}$ emitted in the $\sim \mu s$ delayed annihilation.

In this work the performance of a possible large-acceptance detector for the PHeSCAMI project is investigated using Monte Carlo simulations based on the Geant4 toolkit [7] together with a preliminary characterization of the FB118 material using atmospheric muons and proton beam.

2. Optimization of Trigger logic

The trigger logic of the PHeSCAMI detector is designed to efficiently reject the abundant Minimum Ionizing Particles (MIPs) present in cosmic rays (CRs) while identifying delayed annihilations caused by slow antinuclei stopping in the helium scintillator. This is achieved through a two-step trigger system. The first level of the trigger system, known as the *prompt trigger*, focuses on rejecting MIPs and selecting events where the particles come to a stop inside the detector. Upon satisfying the *prompt trigger* condition, a gate opens for 3.95μs, starting 50 ns after the initial prompt trigger. This gate waits for a *delayed trigger*, which seeks evidence of a delayed annihilation. If the *delayed trigger* condition is met, the event is recorded and stored. The *prompt trigger* leverages the difference in energy deposition between a Z = 1 MIP and a particle that stops within the detector. Stopping particles are slower and experience greater energy losses compared to MIPs. Additionally, MIPs will traverse the entire detector, resulting in four hits in the TOF system, while a stopping particle will produce fewer hits. The *delayed trigger* is designed to detect delayed annihilations of antideuterons $\bar{d}$ and antiprotons $\bar{p}$, which produce secondary pions upon annihilation. The expected number of pions is roughly proportional to the number of annihilating nucleons, with an average of three charged pions for $\bar{p}$ and six charged pions for $\bar{d}$. Consequently, the total energy deposit in both TOF layers and the HeCal is expected to be approximately double for $\bar{d}$ as compared to $\bar{p}$. The topology of the annihilation should result in measurable signals in at least five different scintillator slabs in the TOF.

Prompt Trigger	**Delayed Trigger**
Max E_{dep} outer TOF > 2 $\mathrm{MIP_{TOF}}$	2 $\mathrm{MIP_{TOF}}$ > Max E_{dep} outer TOF > 1 $\mathrm{MIP_{TOF}}$
Max E_{dep} inner TOF > 2 $\mathrm{MIP_{TOF}}$	2 $\mathrm{MIP_{TOF}}$ > Max E_{dep} inner TOF > 1 $\mathrm{MIP_{TOF}}$
Max E_{dep} HeCal > 1.3 $\mathrm{MIP_{HeCal}}$	Max E_{dep} HeCal > 1.3 $\mathrm{MIP_{HeCal}}$
TOF prompt hits $\leq$ 3	TOF delayed hits > 4

Table 1: Summary of the triggers showing discrimination against different energy thresholds, normalized to MIP energy deposition for simplicity. $\mathrm{MIP_{TOF}}$ corresponds to 0.8 MeV and $\mathrm{MIP_{HeCal}}$ to 7.5 MeV. The prompt TOF hits are the number of slabs with an $E_{\mathrm{dep}} > 1\,\mathrm{MIP_{TOF}}$, whilst the delayed TOF hits have an E_{dep} between $\in (1\,\mathrm{MIP_{TOF}}, 2\,\mathrm{MIP_{TOF}})$.

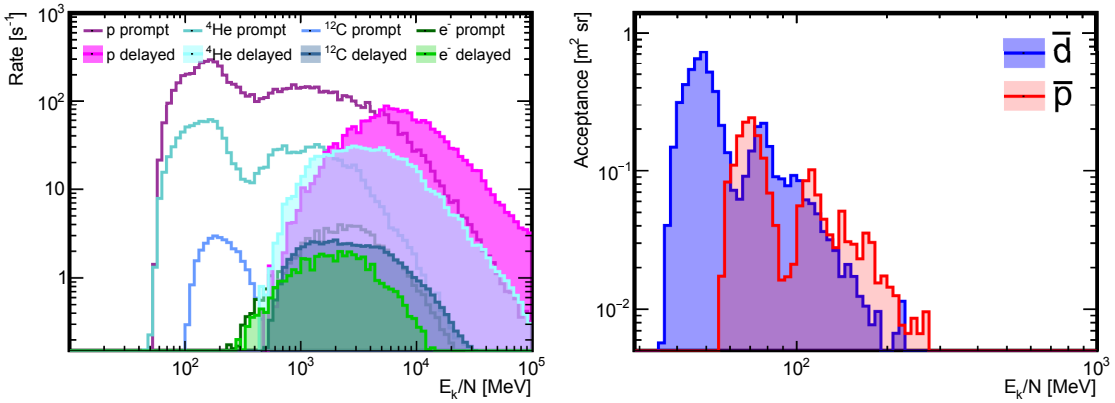

Figure 2: Left: Trigger rates as a function of the kinetic energy per nucleon for p, ^4He, ^{12}C and e^-. Void histograms are the expected prompt trigger rates and filled histograms the delayed trigger rates. Right: trigger acceptances for $\bar{d}$ and $\bar{p}$ as a function of the kinetic energy per nucleon.

3. Background and acceptance

The trigger rate expected for this proposed design of the PHeSCAMI detector is assessed by examining the background from the most prevalent particles and nuclei in CRs. Specifically, protons, ^{4}He, ^{12}C and electrons were simulated with fluxes modeled according to existing measurements [8]. Acceptances are determined by independently applying the two triggers while accounting for pile-up effects within the delayed coincidence gate.

The empty histograms on the left panel of Fig. 2 present the expected rate in each kinetic energy bin for events that satisfy the *prompt trigger*. Similarly, the filled histograms show the expected rates for events satisfying the *delayed trigger*. The expected acquisition rate is computed as the product of the *prompt trigger* rate (9 kHz), the *delayed trigger* rate (2.7 kHz), and the 3.95 μs gate width. Thus, considering the background from ordinary CRs, the expected data acquisition (DAQ) rate is approximately 100 Hz and dead time below 5%. The right side of Fig. 2 presents the expected acceptances of this PHeSCAMI design, with sensitivity to $\bar{d}$ in the range of 40-200 MeV/n and to $\bar{p}$ in the range of 60-250 MeV/n.

4. Antideuterion identification

Following data acquisition, it is essential to process the data to identify potential $\bar{d}$ signatures and separate them from other particle backgrounds. In this preliminary study, we investigate the ability to differentiate $\bar{d}$ from $\bar{p}$. The left panel in Fig. 3 shows the velocity reconstructed by the TOF versus the energy promptly deposited in the HeCal. The right panel in Fig. 3 presents the specific energy loss measured by the external TOF layer against the promptly deposited energy in the HeCal. The energy losses are normalized to the most probable value expected for MIPs, which is 2 MeV/cm. Due to their different masses, for a given energy deposition in the HeCal, the velocity ($\beta = \frac{v}{c}$) of $\bar{d}$ is smaller than that of $\bar{p}$, resulting in higher energy losses. This mass difference facilitates a clear separation between the two particle populations.

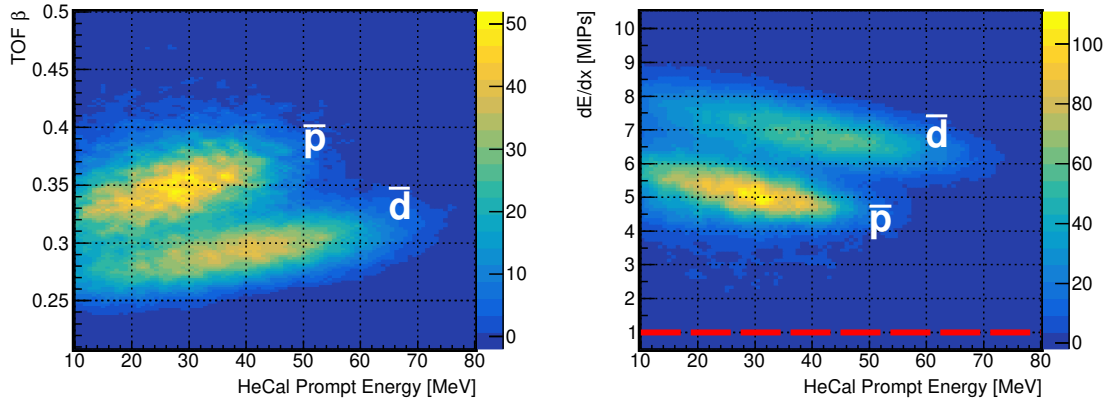

Figure 3: The left panel shows the velocity reconstructed using the TOF versus the energy promptly deposited in the HeCal. The right panel illustrates the specific energy loss measured by the external TOF layer, normalized to the MIP.

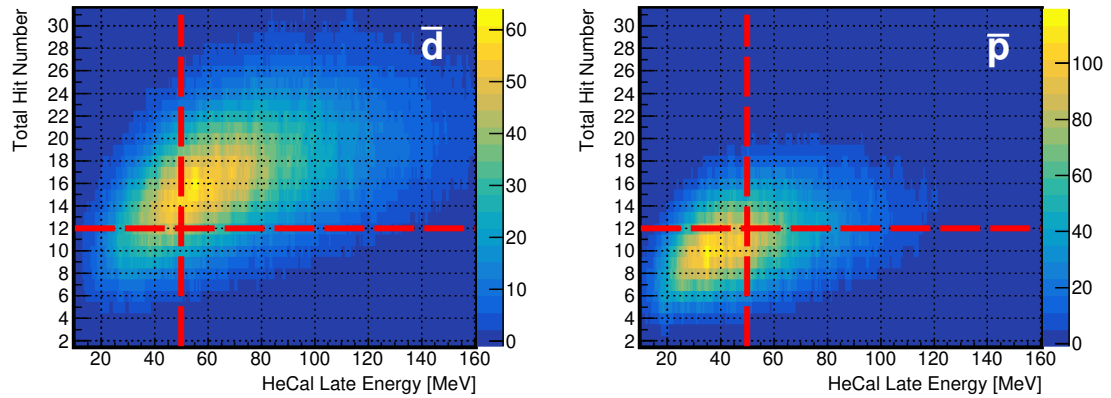

Figure 4: The two panels display the total number of hits (TOF+HeCal) as a function of the energy released by the delayed event in the HeCal. The left panel shows the distribution for $\bar{d}$, while the right panel shows the distribution for $\bar{p}$. For visual aid, the red dashed lines indicate a separation between $\bar{d}$ and $\bar{p}$.

The panels in Fig. 4 display the total number of TOF slabs and helium tanks with signals above the MIP threshold, in the *delayed trigger*, as a function of the delayed energy deposition in the HeCal. The left panel shows the distribution for $\bar{d}$, while the right panel illustrates the results for $\bar{p}$. Due to the higher multiplicity of charged particles produced in $\bar{d}$ annihilations, more hits are generated compared to $\bar{p}$. This provides an additional method for identifying $\bar{d}$ while rejecting $\bar{p}$. The expected separation power will be significantly enhanced with the implementation of a tracking algorithm and multivariate techniques.

5. Development of the HeCal prototype: WLS system

Scintillation light emitted by the helium gas scintillators in the HeCal peaks in the UV range at a wavelength of 80 nm. [5]. To extract this scintillation light from the pressurized vessel, we plan to utilize a design similar to the X-Arapuca, developed for liquid argon (LAr) in the DUNE experiment [6]. In this approach, scintillation photons are downshifted in two stages. First, a

para-Terphenyl (PTP) layer will convert the VUV photons to 350 nm. Next, a PMMA fiber doped with 5-Bis(5-tert-butyl-benzazol-2-yl)thiophene (FB118, manufactured by "Glass to Power" [9] will further shift the light to 425 nm (Fig. 5). As illustrated in Fig. 1, the internal walls of the tank will be coated with PTP, while an FB118 cylindrical fiber will act as an optical window, guiding the light towards an external Photomultiplier Tube (PMT). The subsequent section presents test measurements performed to verify the absence of residual scintillation in FB118, which is crucial to prevent unwanted signals when charged particles inadvertently cross the central fibers of the HeCal.

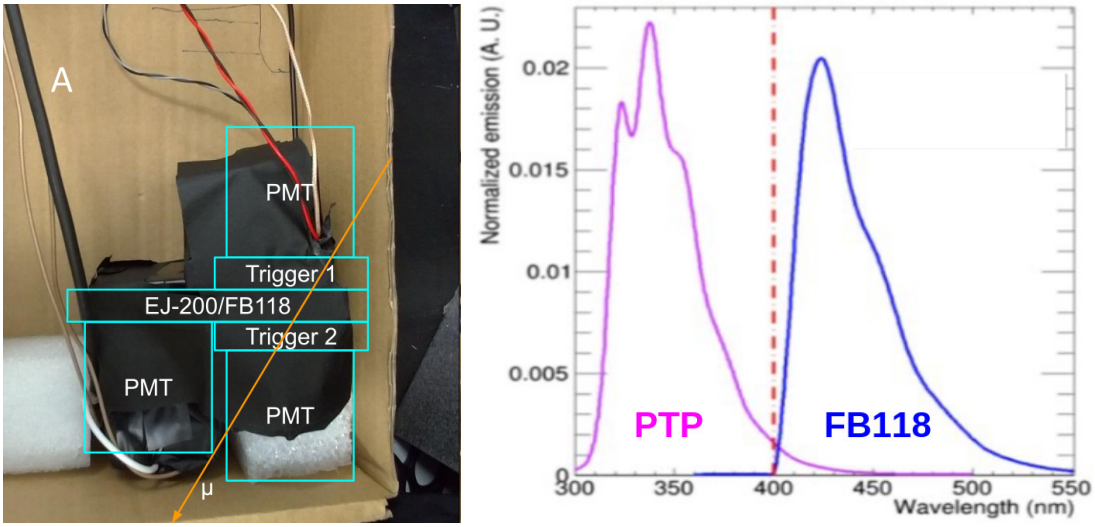

Figure 5: Left: setup for atmospheric muons and proton beam measure of scintillation light of EJ200/FB118. Right: The emission spectra of PTP and FB118.

6. Light yield of FB118

We compared the light yield from a $9\times4\times1$, cm^3 FB118 sample to the signal collected by an EJ-200 plastic scintillator of the same dimensions. The experiment aimed at detecting charged particles was conducted alternatively with the FB118 sample and the EJ-200 control sample, both coupled to the same Hamamatsu R5946 PhotoMultiplier Tube (PMT). The setup included a muon telescope consisting of two additional EJ-200 scintillators (Trigger1 and Trigger2) to detect atmospheric muons passing through the FB118/EJ-200 sample, positioned outside the PMT's cathode (Fig. 5). Without altering the configuration, the same setup was tested with a 74-225 MeV proton beam at the Trento Proton Therapy Center. As two external scintillators triggered the system, there was no minimum threshold for the signal amplitude collected by the FB118/EJ-200 detectors under comparison.

The top panel of Fig. 6 shows the signal amplitude distributions measured with the EJ-200 plastic scintillator when crossed by protons and muons. For the EJ-200 scintillator, the behavior aligns with the Bethe-Bloch formula, where the energy deposition is higher for particles with lower velocity. The bottom panel displays the signal amplitude distributions measured with the FB118 sample. In this case, there is no evidence of light emission induced by protons, suggesting that

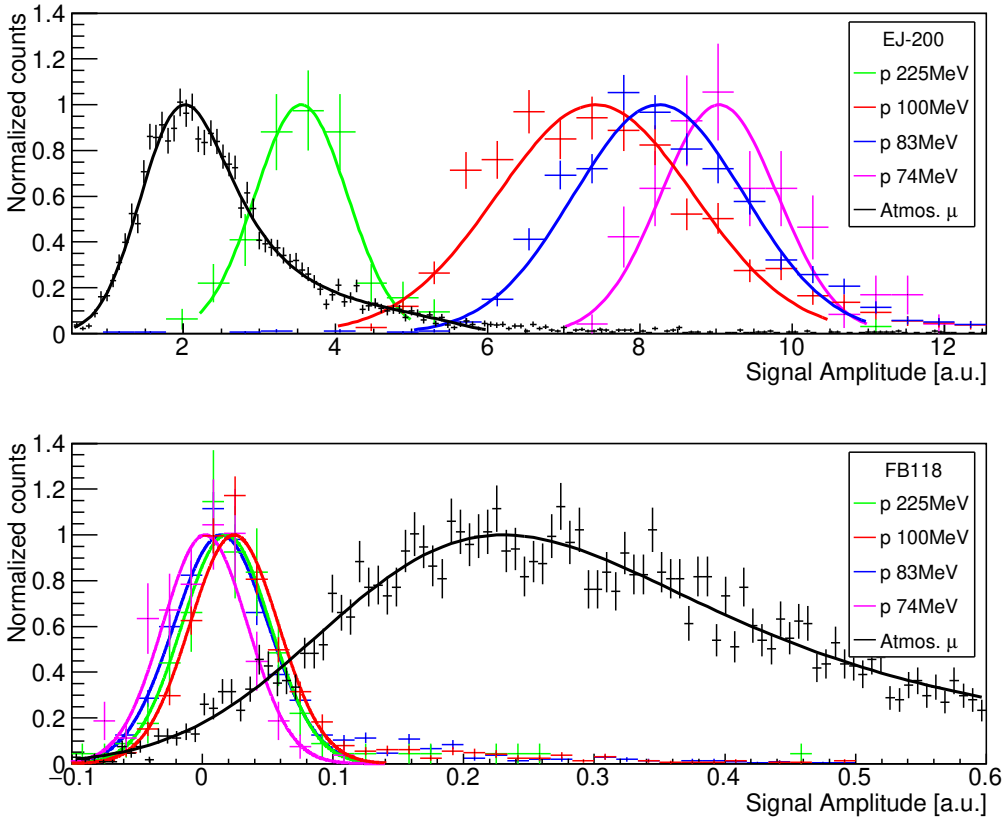

Figure 6: Normalized signal amplitude distributions measured with the EJ-200 scintillator (top panel) and FB118 sample (bottom panel) for protons (green, red, blue, pink) and μ (black). Note the different x-axes scales of the two panels.

the light signal observed with the FB118 sample is mainly due to Cherenkov radiation, given that the expected Cherenkov threshold for protons in FB118 is 310 MeV. Table I summarizes the Most Probable Value (MPV) of the measured distributions for different particle beam tests in both samples. By comparing the signal amplitude distributions for muons in EJ-200 and FB118, we can infer a light yield ratio of $9.1 \pm 0.6(\text{stat.}) \pm 2.5(\text{syst.})$, where the conservative systematic uncertainty was determined by repeating the measurements while varying the PMT, bias voltage, and the PMT optical coupling.

Table 2: MPV of signal amplitudes measured by EJ-200 and FB118 for Protons and μ

Particle	$p\ 74MeV$	$p\ 83MeV$	$p\ 100MeV$	$p\ 225MeV$	μ
MPV EJ-200	9.04 ± 0.08	8.25 ± 0.04	7.42 ± 0.05	3.55 ± 0.06	2.0 ± 0.1
MPV FB118	0.001 ± 0.003	0.014 ± 0.001	0.024 ± 0.001	0.018 ± 0.003	0.22 ± 0.01

7. Conclusion

The simulation of a detector with a wide acceptance, utilizing the PHeSCAMI signature for antideuterons, indicates a maximum geometrical acceptance of $0.7\,\mathrm{m^2sr}$ for $\bar{d}$ and $0.23\,\mathrm{m^2sr}$ for $\bar{p}$. Maximum sensitivity is reached within the energy intervals $E_K/N \in (40, 55)\,,\mathrm{MeV}$ for $\bar{d}$ and $E_K/N \in (60, 75)\,,\mathrm{MeV}$ for $\bar{p}$. Given the proposed design, the predicted DAQ rate due to typical CR background is approximately 100 Hz with ignorable dead time, attributed to the effective rejection capabilities enabled by the unique detection signature. The differentiation of $\bar{d}$ from the $\bar{p}$ background relies on differences in velocity, energy losses, and annihilation topology.

Regarding the WLS system proposed for PHeSCAMI, the light yield of the FB118 WLS material, manufactured by "Glass to Power" [9], was thoroughly investigated. The material does not exhibit scintillation emission, fulfilling the essential requirement for its use as a WLS in the PHeSCAMI project. A high-efficiency Cherenkov emission was observed, reflecting the FB118's capability to convert UV photons into visible light. This effect is not expected to impact the antideuteron identification capability of the PHeSCAMI project, as the region of interest for this detector is limited to $E_k < 300\mathrm{MeV/n}$, which is below the Cherenkov threshold of FB118 ($\beta_{\mathrm{threshold}} \simeq 0.65$).

Acknowledgments

We express our gratitude to A. Pavlovic for providing the FB118 sample. This research was supported by the Italian Ministerial grant PRIN-2022, project number 2022LLCPMH, titled "PHeSCAMI-Pressurized Helium Scintillating Calorimeter for AntiMatter Identification,"
CUP E53D23002100006.

References

[1] S. S. Adler and et al. (PHENIX Coll.), "Deuteron and Antideuteron Production in Au + Au Collisions at $\sqrt{s_{NN}} = 200$ GeV," *Phys. Rev. Lett.*, vol. 94, p. 122302, Apr 2005.

[2] S. Acharya and et al. (ALICE Coll.), "Measurement of anti-3He nuclei absorption in matter and impact on their propagation in the Galaxy," *Nature Physics*, vol. 19, p. 61–71, Dec. 2022.

[3] F. Nozzoli, I. Rashevskaya, L. Ricci, F. Rossi, P. Spinnato, E. Verroi, P. Zuccon, and G. Giovanazzi, "Antideuteron Identification in Space with Helium Calorimeter," *Instruments*, vol. 8, no. 1, 2024.

[4] MT Areospace AG, *https://www.mt-aerospace.de/downloads.html*.

[5] R. E. Huffman, J. C. Larrabee, and D. Chambers, "New Excitation Unit for Rare Gas Continua in the Vacuum Ultraviolet," *Appl. Opt.*, vol. 4, pp. 1145–1150, Sep 1965.

[6] C. Brizzolari and et al., "Enhancement of the X-Arapuca photon detection device for the DUNE experiment," *Journal of Instrumentation*, vol. 16, p. P09027, Sept. 2021.

[7] S. Agostinelli and et al. (GEANT4 collaboration), "Geant4—a simulation toolkit," *Nuclear Instruments and Methods in Physics Research Section A: Accelerators, Spectrometers, Detectors and Associated Equipment*, vol. 506, no. 3, pp. 250–303, 2003.

[8] D. Maurin and et al., "A cosmic-ray database update: CRDB v4.1," *The European Physical Journal C*, vol. 83, Oct. 2023.

[9] " Glass to Power - Luminescent Solar Concentrators. https://www.glasstopower.com."